JARO 02: 279–296 (2001)
DOI: 10.1007/s101620010069

JARO
Journal of the Association for Research in Otolaryngology

Laminar Analysis of Inhibition in the Gerbil Primary Auditory Cortex

ELISABETH FOELLER,[1] MARIANNE VATER,[2] AND MANFRED KÖSSL[1]

[1]*Zoologisches Institut, Universität München, München, Germany*
[2]*Institut für Biochemie und Biologie, Universität Potsdam, Potsdam, Germany*

Received: 31 July 2000; Accepted 7 April 2001; Online publication: 1 August 2001

ABSTRACT

Physiological and immunocytochemical evidence indicates a layer-dependent organization of inhibitory circuits in the neocortex. To investigate the contribution of GABAergic inhibition to frequency tuning in the different cortical layers, we recorded single and multiple units in near-radial penetrations before and during iontophoretic application of the $GABA_A$-receptor antagonist bicuculline in the auditory cortex of the lightly anesthetized gerbil. Bicuculline generally increased the spontaneous rate and enhanced and prolonged onset activity. Application of bicuculline often resulted in a shift of best frequency and a decrease of threshold (5.5 dB). A broadening of the frequency tuning evident by lower Q_{40dB} values was observed in 63% of the units. In units with multipeaked tuning curves or clearly separated response areas, bicuculline application removed the inhibitory regions and created single-peaked tuning curves. The influence of bicuculline on the receptive field size was not significantly layer-specific but tended to be most pronounced in layers V and VI. In layer VI, we frequently found "silent" neurons that responded to sound only when GABAergic inhibition was antagonized. From the analysis of postembedding GABA immunocytochemistry, the proportion of GABAergic neurons was found to be maximal in layers I and V, and the number of GABAergic perisomatic puncta (axon terminals) on cell somata peaked in layer V.

Correspondence to: Dr. Elisabeth Foeller · Zoologisches Institut · Universität München · Luisenstr. 14 · 80333 München, Germany. Telephone: 49-89-5902-202/608; fax: 49-89-5902-450; email: foeller@zi.biologie.uni-muenchen.de

Keywords: auditory cortex, inhibition, bicuculline, GABA, immunocytochemistry

INTRODUCTION

Neurons along a path perpendicular to the cortical surface often share similar response characteristics and these properties vary systematically across the cortical surface. Columnar organization is a common feature of cortical architecture (Mountcastle 1997). In the visual cortex, systems of columns are well documented for ocular dominance, orientation selectivity, and spatial frequency. In the auditory cortex, there is ample information about topographic organization in the form of tonotopic frequency gradients (e.g., cat: Merzenich et al. 1975; mustached bat: Suga and Jen 1976; owl monkey: Imig et al. 1977; albino rat: Sally and Kelly 1988; gerbil: Thomas et al. 1993) or binaural maps (e.g., Imig and Adrian 1977; Phillips and Irvine 1983).

Much less is known about a functional vertical organization within columns in the auditory cortex. Neurons recorded during perpendicular penetrations exhibit similar best frequencies (Oonishi and Katsuki 1965; Abeles and Goldstein 1970; Sugimoto et al. 1997; Shen et al. 1999). Field potential recordings revealed a sequential activation of the supragranular and then the infragranular pyramidal cells in laminar circuitry of the rat auditory cortex suggesting a hierarchically organized processing of receptive field information (Barth and Di 1990). On the level of single neuron recordings, Oonishi and Katsuki (1965) reported that, with increasing depth, the sharpness of tuning curves

of cat auditory cortex neurons increased and suggested an integrative mechanism from deeper layers to the superficial layers. In contrast, Volkov and Galazjuk (1991) found that tuning sharpness decreased with cortical depth. Furthermore, no statistically significant evidence for a layer-dependent sharpness of tuning was observed by Abeles and Goldstein (1970). No change of tuning with recording depth was reported for the mouse auditory cortex (Shen et al. 1999). Sugimoto et al. (1997) found increased tuning sharpness in layers III and IV of the gerbil primary auditory cortex (A1) and concluded that the laminar differences of the receptive field size were mainly determined by the highly specific afferent input in A1. A possible explanation for these divergent results may be found in the fact that receptive field size is determined by intracortical inhibition, which could vary considerably depending on the stimulation procedure and anesthesia. Layer-dependent differences in tuning sharpness could be a consequence of either specific thalamocortical input or of layer-specific intracortical inhibition. Laminar differences in the geometry of dendritic trees (e.g., Mitani et al. 1985) and neuronal connections (e.g., Prieto et al. 1994a, b) might indicate a possible difference in the integration of excitatory and inhibitory inputs in specific layers.

Neurons containing γ-aminobutyric acid (GABA) and GABA receptors are conspicuous elements of cortical organization (review for the auditory cortex: Winer 1992). In immunocytochemical studies of the cat auditory cortex, GABAergic neurons and axon terminals were identified and localized (Prieto et al. 1994a, b) and a layer-specific distribution of the percentage of GABA-immunopositive cells and axon terminals was observed. GABAergic neurons serve to regulate overall cortical excitability and neuronal population synchronization (e.g., Avoli et al. 1994; Tamás et al. 2000) and are involved in shaping neuronal receptive fields and response profiles. For example, GABAergic inhibition controls the orientation selectivity of neurons in the visual cortex (e.g., Sillito 1984; Crook et al. 1998) and the receptive field size of neurons in the somatosensory cortex (cat: Dykes et al. 1984; whisker barrel cortex of rat: Kyriazi et al. 1996).

Several studies investigated the influence of inhibition in the auditory cortex using forward or simultaneous masking (e.g., Shamma et al. 1993; Calford and Semple 1995; Brosch and Schreiner 1997; Sutter et al. 1999). In these experiments, the suppressive influence of masker tones of different frequencies on a fixed probe tone at a given frequency within the cells' excitatory response area was measured. The masker was presented either at the same time (simultaneous) or prior to (forward) the probe tone. The origin of the inhibition seen in these masking studies was unclear since the investigated cortical neuron received excitatory afferents whose response characteristics were already shaped by excitation and inhibition in lower stages of the auditory pathway.

Several studies have looked directly at the effects of GABA inhibition on the response features of auditory cortical cells to other auditory stimuli as well. In the bird auditory cortex, GABA-mediated inhibition increases neuronal selectivity to natural sounds and sharpens frequency tuning (Müller and Scheich 1987, 1988). Horikawa et al. (1996) showed that optically recorded excitatory bands are surrounded by GABA-mediated inhibitory areas in the guinea-pig auditory cortex. Recently, Wang et al. (2000) demonstrated that removal of GABA-mediated inhibition results in lower threshold, an increase in discharge rate, and a broadening of excitatory receptive fields in the chinchilla A1. In the gerbil, there are massive effects of $GABA_A$ antagonists on overall neuronal activity in the auditory cortex as viewed by deoxyglucose mapping (Richter et al. 1999). Schulze and Langer (1999) investigated the influence of blocking GABA-mediated inhibition on the response of A1 neurons in the gerbil and concluded that GABA sharpens neuronal amplitude-modulation tuning.

The aim of this study was to examine the functional role of intracortical inhibition in frequency tuning of single and multiple units in the gerbil primary auditory cortex by iontophoretic application of the $GABA_A$-receptor antagonist bicuculline (BIC) and to investigate a possible layer-specific effect of inhibition on the frequency tuning.

MATERIALS AND METHODS

Neurophysiology

Surgical procedure. Experiments were performed on 21 male and female adult gerbils (*Meriones unguiculatus*; body weight between 50 and 80 g). For initial surgery, animals were anesthetized with an intramuscular injection of a 10:1 mixture of ketamine (130 mg/kg) and xylazine (Rompun 2%, Bayer). During the experiments, light anesthesia was maintained by a continuous infusion of the anesthetic administered subcutaneously by a Harvard Apparatus Infusion Syringe Pump 22 (20–40 mg/kg/per hr). Light anesthesia was monitored using the pedal-withdrawal reflex in regular intervals and observation of breathing patterns. The body temperature of the animals was maintained at 37°C by a heating pad. Recording sessions lasted up to 18 hours. After the experiments were completed, the animals were killed with an overdose of pentobarbital sodium. All experiments were conducted in a sound-shielded chamber.

The animal's head was fixed by a metal bar cemented on the skull with dental cement. The temporal muscle on the left hemisphere (right hemisphere in 4 animals) was retracted and the lateral cortex was exposed by a craniotomy. The overlying dura was incised and reflected, and the cortex was covered with either paraffin oil or physiological saline solution throughout the experiment.

Neurophysiological recording. Prior to microiontophoretic application of drugs, the location of the primary auditory cortex was determined by the position of the cortical vasculature (Thomas et al. 1993; Sugimoto et al. 1997) and by recordings of multiple units or local field potentials at slightly different rostrocaudal positions and comparing the measured frequency gradient with a frequency map of the gerbil A1 (Thomas et al. 1993).

"Piggyback" multibarrel electrodes (Havey and Caspary 1980) were used for recording and iontophoretic drug application. The tip of a 4-barrel glass pipette was broken to a total diameter of 8–15 μm. A single-barrel recording electrode was glued onto the multibarrel pipette such that its tip protruded about 5–15 μm beyond the tip of the multibarrel. One barrel of the multibarrel electrode was used for balancing currents and was filled with 1 M NaCl. The other 3 barrels were filled with the $GABA_A$-receptor antagonist bicuculline-methiodide (5 mM, pH 3, Sigma, St. Louis, Mo), GABA (0.5 M, pH 3.5, Sigma) or glutamate (1 M, pH 8, Sigma). A microiontophoresis system (S7061A, WPI, Sarasota, FL) was used to generate and monitor ejection currents (BIC, GABA: 2 to 60 nA; glutamate: −5 to −10 nA) and retention currents (BIC, GABA: −8 to −15 nA, glutamate: 10 to 15 nA). The recording electrode was filled with 3 M KCl (resistance *in situ*: 3–10 MΩ). Using a piezo-microdrive, the piggyback electrode was lowered in a direction perpendicular to the cortical surface to record multiple and single units in cortical layers I to VI. The electrical signal from the recording electrode was amplified, band-pass filtered (0.3–3 kHz; Stanford SR650), and fed into a window discriminator (custom-made). Signals were A/D converted and stored on the computer.

During near-radial penetrations, the recorded units could be assigned to cortical layers by means of cortical depth. The extents of the six auditory cortex layers were analyzed in two brains stained for Richardson blue and Nissl and were found to be comparable to data from Sugimoto et al. (1997): layer I: 0–120 μm; layer II: 120–210 μm; layer III: 210–410 μm; layer IV: 410–560 μm; layer V: 560–850 μm; layer VI: 850–1300 μm.

Acoustic stimulation. Pure tone stimuli (50–100 ms duration, 4 ms rise/fall time) were generated by a synthesizer (HP 8904 A), gated, and fed through an attenuator (Jim Hartley, custom-made) into the calibrated loudspeaker (1/2-in. B&K 4133 microphone capsule, Bruel & Kjaer, Norcross, GA). A tube fixed on the speaker was tightly sealed into the auditory meatus. To obtain frequency response areas, pure tones of various frequencies and intensities (duration: 80–100 ms) were randomly presented with interpulse intervals of 400–500 ms. Each frequency–intensity combination was presented 10 times and corresponding neuronal responses were averaged. Twenty-four or 32 logarithmically spaced frequencies spanned 3–8 octaves centered on the approximate best frequency (BF: frequency to which neurons responded at lowest intensities). Usually a 5-octave range was used which provided a 0.2–0.16-octave resolution between frequencies. Sound pressure levels covered a total range of 80 dB.

Data analysis. From the frequency response area, a software routine calculated the frequency tuning curve, the BF, the threshold at BF, and the Q_{10dB} and Q_{40dB} values (the best frequency of a neuron divided by the bandwidth of the tuning curve 10 dB or 40 dB above threshold). To obtain comparable tuning curves under control and drug condition, we used a method similar to that of Sutter and Schreiner (1991) and Sutter et al. (1999). The maximum driven spike rate and the spontaneous activity were included in the threshold criterion used for defining tuning curves because bicuculline increased both activity components. The response threshold was defined as 20% maximal stimulus-evoked onset discharge rate plus the spontaneous activity calculated in an equally long time window. The onset discharge rate was used because in the majority of the cells, the onset discharge was followed by an inhibitory period that considerably reduced the spike discharge rate during the stimulus duration. The onset time window was individually adjusted to each unit because latency and duration of the onset discharge rate varied among units, e.g., units exhibiting bursting activity showed prolonged onset discharge duration. Accordingly, the used measurement window varied between 20 and 30 ms. The spontaneous rate was calculated from the averaged spike rate measured during the whole record duration for at least 12 frequency-level combinations for which no obvious driven discharge rate was observed. For example, in Figure 1A the neuronal activity during the first eight frequency steps (1.7–3.7 kHz) at the two lowest levels (−10 and −5 dB SPL) was classified as "spontaneous" and used to derive the spontaneous activity value.

The first spike latency of single neurons, which is defined as the latency of that spike in a PST histogram that occurs first after onset of the stimulus, was analyzed before and during BIC application 10–20 dB above the actual threshold. In 8 out of 57 neurons that

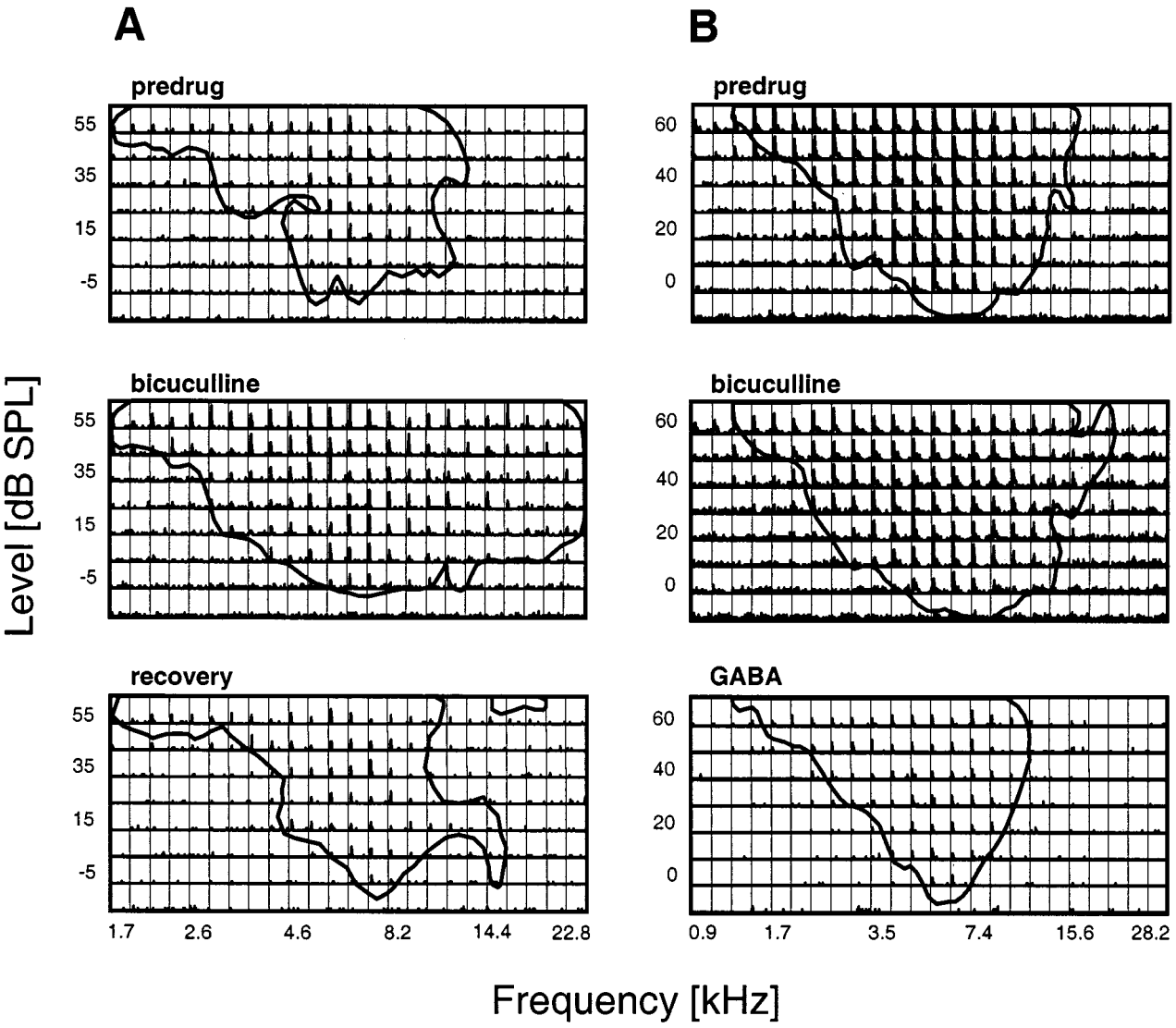

FIG. 1. **A**. Tuning curves and PST histograms for a single unit in layer V in response to random presentation of a 80-ms pure tone at frequencies from 1.7 to 22.8 kHz and intensities from −25 to 55 dB SPL before (*top*), during (*middle*), and after (*bottom*) the application of BIC (5 nA). Each box represents the average of neuronal activity over 10 trials and over 240 ms for each frequency-level combination. PSTH bin width is 4 ms. PSTH *y* axis is 12 spikes. Threshold criterion for the tuning curves is 20% maximum onset spike rate plus spontaneous activity. **B**. Example for a single unit in layer III for which no change of the receptive field was measured during the application of BIC (10–20 nA) despite an increase in spontaneous activity. Application of GABA (20 nA) decreased the spontaneous activity and the receptive field size was reduced slightly. Each box represents the average of neuronal activity over 8 (*top*/*middle*) and 4 (*bottom*) trials over 240 ms for each frequency–level combination. PSTH bin width is 4 ms. PSTH *y* axis is 20 spikes (*top*/*middle*) and 10 spikes (*bottom*).

could be measured before and during BIC application, the response was extremely variable because of a low spike probability (<30%) before BIC application and, hence, the latency was unreliable. Because of the high response variability, these units were excluded from the analysis of a latency shift caused by BIC.

Immunocytochemistry

Two adult animals were deeply anesthetized by intraperitoneal injection of a 10:1 mixture of ketamine (350 mg/kg) and xylazine (Rompun 2%, Bayer), then perfused through the heart at 4 mL/min with saline (5 min) followed by a fixative (2.5% glutaraldehyde in 0.1 M phosphate buffer, 40 min). The brain was removed and postfixed overnight at 4°C. Frontal sections 200 μm thick and containing the primary auditory cortex (2–3 mm rostral of Lambda) were cut on a vibratome, osmicated, dehydrated, and embedded in Durcupan. Alternating series of semithin sections (1 μm) were collected; one series was stained with Richardson blue and the other was used for GABA

immunostaining (antibody obtained from SFRI, France). Immunocytochemistry basically followed the protocols given by Liu et al. (1989) and Kolston et al. (1992). Detailed protocols for GABA immunostaining can be found elsewhere (Vater 1995; Kemmer and Vater 1997).

For quantitative analysis, immunostained sections, and adjacent Richardson blue-stained sections were light microscopically analyzed with a Leitz Dialux 20 attached to an image processing system. To determine the percentage of GABA-immunopositive neurons, cell counts were performed in semithin (1 μm) sections from two 200-μm-thick slabs. For each slab, three semithin sections with a 20-μm interval between sections were studied. In each section two columns running from the pia to the white matter were analyzed from videoprints obtained with a magnification of $\times$400. After establishing layer boundaries, all nucleated neuronal profiles were counted in 12 sample areas per layer (300 μm wide and 100 μm high; layer II: 300 μm wide and 75 μm high).

To estimate the laminar distribution of GABAergic axon terminals, immunopositive puncta on cell somata were examined with an objective (N.A. 1.25, $\times$100) under oil immersion. In layers I and IV, puncta on nonpyramidal cells and in layers II, III, V, and VI, puncta on pyramidal cells were counted. Profiles were classified as puncta when they were either round or oval and did not resemble cross-sectioned dendrites or axons (Prieto et al. 1994b).

RESULTS

Extent of diffusion of bicuculline in the auditory cortex

There are some difficulties in interpreting results obtained by iontophoretic application of pharmacologically active compounds (Hicks 1983), especially bicuculline. Its removal from the tissue appears to be dependent on the diffusion rate, and the effect of BIC could take as long as 20 minutes to disappear as measured in our study. Because of time constraints, a full recovery of the drug effect was not always achieved and, therefore, during a penetration through the cortex, BIC could accumulate. To gain insight into the extent of the diffusion and time course of clearance of BIC within the cortical tissue, we applied BIC in one animal using single-barrel electrodes (tip diameter = 3 μm) separated several 100 μm from the recording injection pipettes and measured the effect of the drug at different current levels. The influence of BIC at the recording site was tested in a multiple unit in layer III and in four single units in layer V. A pure tone at the best frequency and 20 dB above threshold was presented (stimulus duration of 80 ms, interpulse interval of 800 ms). From responses to 40 presentations of this tone, the overall spike rate was calculated. This procedure was repeated 5 times during a time interval of 5 minutes. An average spike rate and the standard deviation were calculated from the 5 measurements. Then, BIC was applied at ejection currents of 10, 20, 30, and 40 nA. At each current level, the response rate was measured with the same measurement procedure as under predrug conditions; the drug was applied continuously while the units' response was recorded. If, at a given current level, there was no effect of BIC after 10 minutes of drug injection, we increased the injection current to the next higher level. BIC was considered to have a significant effect at a particular current level when the spike rate increased to a value of the mean spike rate plus two times the standard deviation measured during the control situation.

In layers III and V, an ejection current of 30 nA increased the spike rate of a cell that was 150 μm away from the injection site, while a 40-nA current increased spiking in a cell 350 μm from the BIC injection. At a distance of 400 μm, one unit was affected after 5 minutes at 40 nA, while another was not affected after 10 minutes. We conclude that for the ejection currents commonly applied in our experiments (10–40 nA), locally applied BIC can influence responses of neurons located at distances of up to approximately 400 μm. Effects of BIC caused by diffusion could take several minutes. We recorded only from units that showed a fast effect to drug application. Therefore, we measured local effects and possibly—during the time course of the tuning curve measurement (13–17 min)—diffusion effects. We cannot rule out the possibility that those units that were recorded in a sequence and were spaced less than approximately 400 μm were under the influence of elevated levels of BIC. Thus, we measured the net effect of BIC on a small network of cells. To minimize such indirect effects of BIC, the drug was applied at the lowest effective ejection currents and a waiting period of at least 10 minutes was interspersed between data collection from different units.

General effects of bicuculline

We recorded 88 multiple units and 64 single units from 21 gerbils in 22 near-radial penetrations. The number of units recorded in a penetration varied between 3 and 14. The variability of BF with depth could be analyzed in 20 penetrations where units were recorded over a depth range of at least 600 μm. According to Sugimoto et al. (1997) and Merzenich et al. (1975), we estimated the variability of BF within each penetration using the fractional bandwidth, which is defined as

the ratio of the difference of the maximum BF and minimum BF encountered to the minimum BF. Fourteen penetrations showed a fractional bandwidth of ≤1 (0.1–1.0) and were defined as exhibiting nearly constant BF with depth. In the remaining 6 penetrations, 1 or 2 units out of 6–8 units per penetration showed a different BF which caused higher fractional bandwidth of 1.3–3.8.

Once a unit was isolated, its frequency response area was measured. Then, BIC was iontophoretically applied with increasing ejection currents until an increase in spontaneous or evoked discharge activity was observed, which occurred at 10–40 nA for most units. The increase in discharge rate usually occurred rapidly (within 1–2 minutes) and was stable for several minutes. The ejection current was not increased further to prevent the tissue from being saturated with BIC and to ensure a local application of the drug. BIC was applied continuously during the measurement of the receptive field. In the majority of the units, the recordings were stable for more than one hour, and, hence, it was possible to measure recovery from BIC or to additionally investigate the effect of GABA.

BIC increased the spontaneous firing rate in 82% of the units tested at ejection currents between 2 and 60 nA. The mean increase in spontaneous rate of these units amounted to 235% (range 6%–3780%; units that showed no or <0.1-spike/s spontaneous activity before BIC application were excluded from this analysis). In most cortical units, the tone-evoked response consisted of a phasic increase of discharge rate related to stimulus onset. This onset activity, measured in a 20–30-ms time window starting with the first stimulus-evoked spike, was increased in 79% of the units for stimulus levels of up to 80 dB SPL. The mean increase in stimulus-evoked discharge rate of these units amounted to 147%.

Influence of bicuculline on receptive fields of single and multiple units

For 127 units, a tuning curve could be calculated before and during application of BIC. The influence of BIC on frequency tuning curves of a single unit in layer V is shown in Figure 1A. Under control conditions (predrug, *top*) the spontaneous activity was 2.3 spikes/s and increased to 6.1 spikes/s during the application of BIC (*middle*). The maximum onset discharge rate increased from 17 spikes (at 5.8 kHz, 55 dB SPL) to 33 spikes (at 5.2 kHz, 35 dB SPL) during BIC iontophoresis. A broadening of the receptive field toward higher frequencies was observed and Q_{10dB} and Q_{40dB} values decreased during BIC application (predrug: 2.3 and 0.9; BIC: 0.85 and 0.35). A recovery of the drug effects was achieved immediately after finishing drug ejection (*bottom*).

In general, BIC enlarged the receptive field. The degree and the form of the enlargement were various and complex. Figures 2A and B show two further examples of single units in layers V and II for which the application of BIC led to a pronounced broadening of the frequency tuning curve at the low-frequency and the high-frequency sides of the tuning curve. This demonstrates intracortical GABAergic inhibition creating inhibitory sidebands that surround the excitatory response area. In addition, the threshold of the neuron shown in Figure 2A decreased during the application of BIC suggesting that inhibition was also present within the excitatory receptive field. The broadening of the tuning curve was often more pronounced at high sound levels than at low levels (e.g., Fig. 2D).

To gain an insight into possible unspecific changes of BF over time, we compared the BF of the tuning curves measured before and after BIC application (recovery). In 34% of the investigated units (n = 15), a shift of the BF of ≥0.2 octave was observed, the maximal individual shift amounted to 0.47 octave. In the remaining 66% of the units the BF did not shift, as assessed by using the 0.2-octave criterion. During application of BIC, a shift of BF of the units to higher (27%) or lower frequencies (39%) was observed. The remaining 34% of the units showed no apparent change of their BF. For the majority of the units, the shift of BF was below 1 octave, but 10 units shifted their BF by more than 1 octave to lower frequencies (Fig. 2C) and 4 units shifted their BF by more than 1 octave to higher frequencies (maximum shift of 2.5 octaves). Thresholds of different units varied between −12 and 45 dB SPL prior to drug application. BIC decreased the threshold in 63% of the units (e.g., Figs. 2C and D). The average decrease was 5.5 ± 4.8 dB. We suggest that this decrease of threshold was caused by a release of inhibition since unspecific threshold changes, assessed from the differences measured before and after BIC application (recovery), did not show a systematic decrease and were on average −0.12 ± 5.4 dB (n = 15).

Eleven units exhibited multipeaked frequency tuning curves in control conditions; the most extreme case is shown in Figure 2E. This multiple unit in layer VI had four clearly separated response areas that were merged during BIC application creating a very wide tuning curve. Similar effects were also seen in four single units. BIC eliminated receptive field gaps at higher stimulus levels. This demonstrates the involvement of intracortical GABAergic inhibition in the creation of nonmonotonic rate-level functions (Fig. 2F).

An example for a single unit for which the receptive field structure did not change remarkably during $GABA_A$ blockade, although BIC increased the spontaneous activity from 15 to 40 spikes/s, is shown in Figure

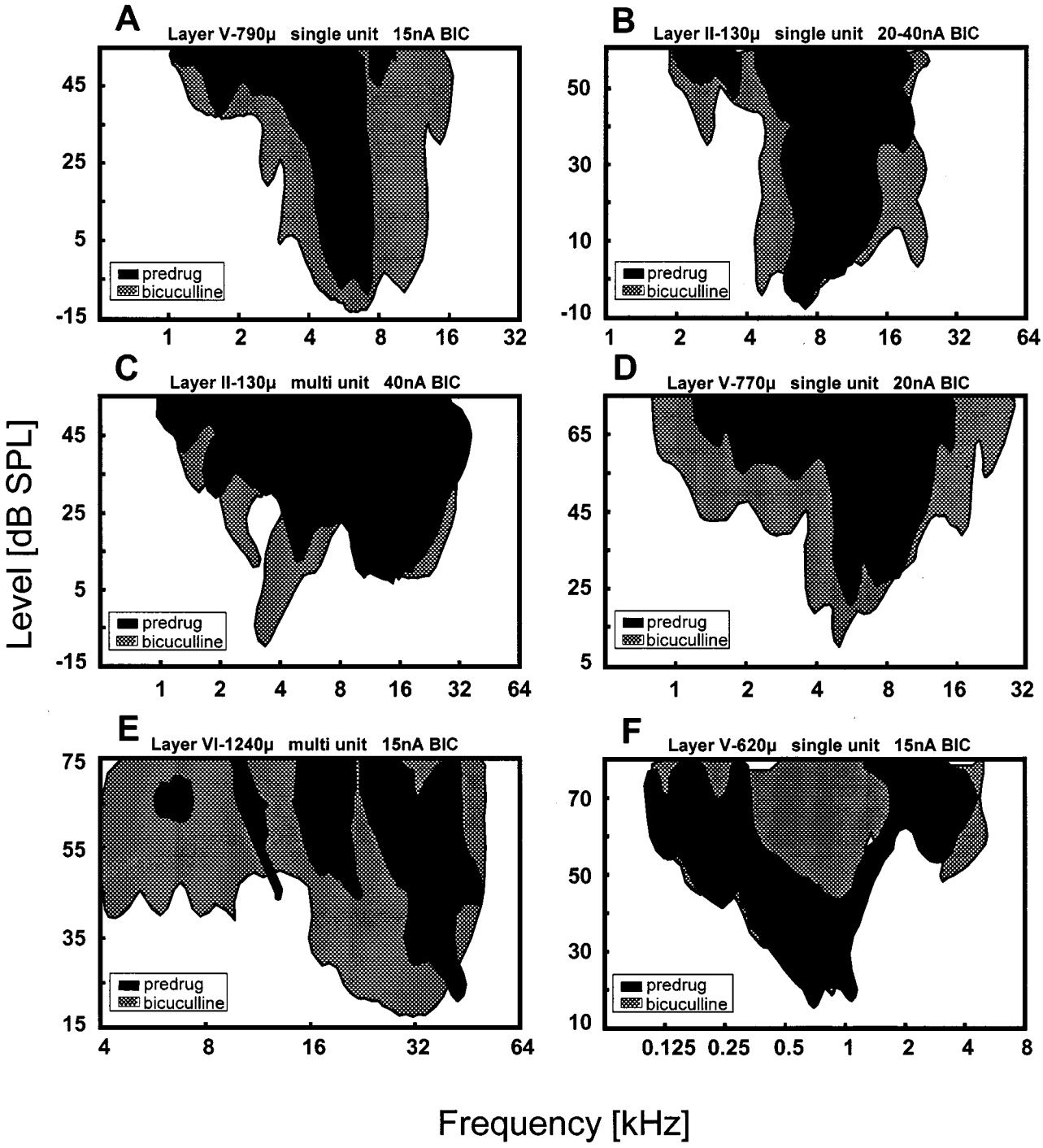

FIG. 2. Examples for receptive fields of single and multiple units from different layers under predrug condition (black) and during the application of BIC (gray).

1B. GABA application reduced the spontaneous rate to 1.25 spikes/s and shifted the high-frequency slope of the receptive field downward by about 2 kHz.

Influence of bicuculline on the tuning sharpness

Changes of tuning sharpness as a result of the blockade of GABAergic inhibition were analyzed in all units that showed an increase of spontaneous and/or stimulus-evoked activity during the application of BIC. The correlation of tuning sharpness expressed as Q_{10dB} and Q_{40dB} before and during the application of BIC is plotted for single and multiple units (Fig. 3). In the control situation, the mean Q_{10dB} was 2.3 (n = 127; range = 0.6–5.8) and slightly decreased to 2 during BIC application (range = 0.5–7.8). The decrease of Q_{10dB}

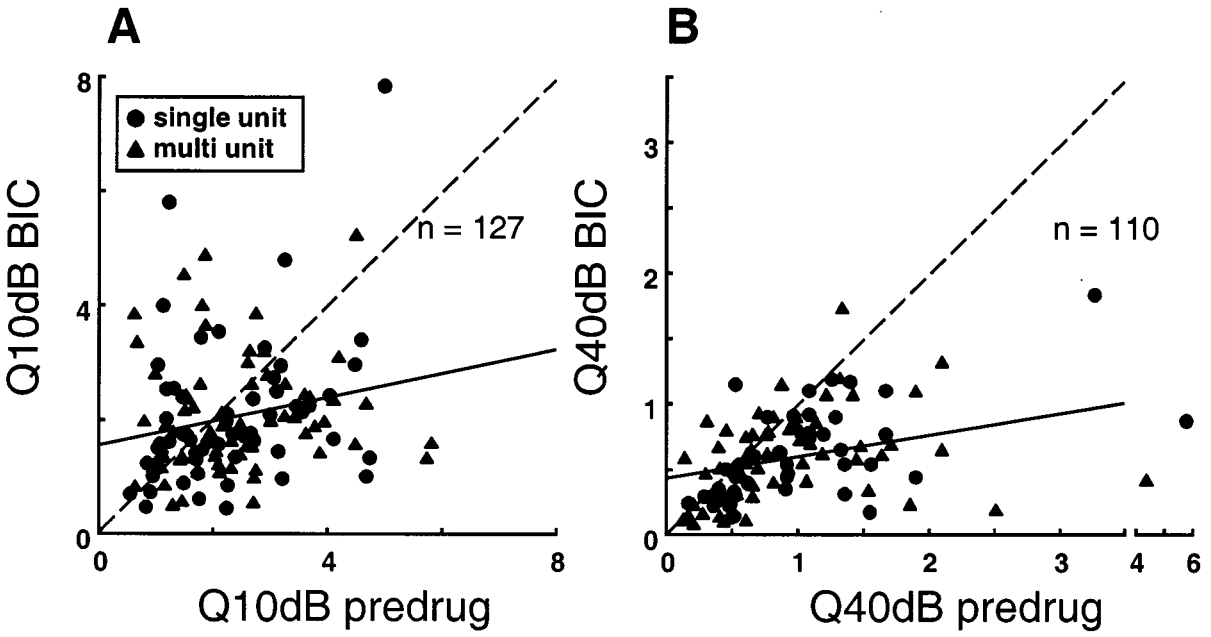

FIG. 3. Correlation between Q values of tuning curves before and during BIC application with regression lines. Equal Q values before and during BIC application result in a point on the dashed line at 45°. **A**. Q_{10dB} with $y = 0.21x + 1.56$ ($r = 0.21$). **B**. Q_{40dB} with $y = 0.16x + 0.43$ ($r = 0.38$). Both correlations were significant ($p < 0.05$; $p < 0.01$).

was significant ($p < 0.01$, paired 2-tailed Wilcoxon test). If we defined tuning curves as narrow when their Q_{10dB} value was >2 (Pelleg–Toiba and Wollberg 1989), then the percentage of narrowly tuned units decreased from 54% before BIC to 41% during BIC application. The mean Q_{40dB} decreased from 1 (range = 0.1–6) during predrug conditions to 0.6 (range = 0.1–1.8) during BIC application. The decrease of the Q_{40dB} was highly significant ($p < 0.001$, paired 2-tailed Wilcoxon test). Before drug application 75% of the units ($n = 110$) had values >0.5 compared with 56% during BIC application. The total sample is smaller for the Q_{40dB} values because in some units threshold was relatively high and we did not measure 40 dB above threshold, or the bandwidth was not clearly defined because the flanks exceeded the frequency boundaries of the measurement.

Effects of bicuculline across different cortical layers

By using near-radial penetrations, it was possible to study BIC effects in different cortical layers, defined by the depth of the recording site. General physiological response properties varied among layers, for example, cells in layers II and IV were characterized by low spike amplitudes, whereas in layers III, VI, and, in particular, layer V, numerous single units with large spike amplitudes were isolated that often showed bursting activity.

Examples for the depth-dependent distribution of the BF are shown in three near-radial penetrations before and during BIC application (Fig. 4). In 13 out of 20 penetrations, the BF remained nearly constant with recording depth (fractional bandwidth ≤1) and was similar during BIC application (Fig. 4A). In a penetration that was likely to be at the border between A1 and the anterior auditory field, where units were exceptionally broadly tuned, BIC shifted the BF downward in layers III and IV (Fig. 4B). For the penetration shown in Figure 4C, BIC stabilized the BF at values below the predrug condition for all layers. In the remaining 5 out of 20 penetrations where we could record enough units to analyze a dependence of BF with depth (fractional bandwidth >1), the BF during BIC either was similar to the BF during predrug conditions or no regular changes caused by the application of BIC were found.

Latency of single units. Stimulus-evoked first spike latency of single units, before and during BIC application, was analyzed 10–20 dB above the actual threshold at the BF. Ranges of latencies were between 16 and 40 ms before and between 12 and 41 ms during the application of BIC. The mean latencies were similar across the different layers (Fig. 5). Slightly shorter latencies were found in layer VI, but this difference was not significant (t-test, $p > 0.05$). The change of latency caused by BIC was highly variable between neurons (range = −12 to 12 ms, average = −0.98

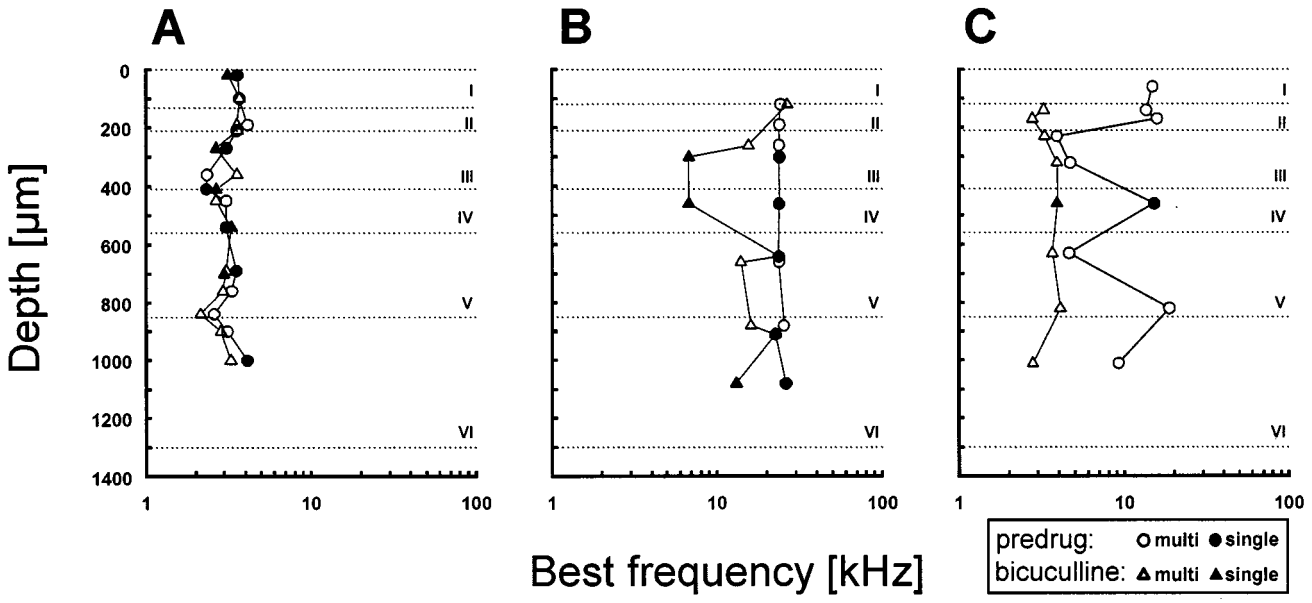

FIG. 4. Depth-dependent distribution of the best frequency during three near-radial penetrations in three animals before (circles) and during (triangles) BIC application. Open symbols represent multiple units; closed symbols represent single units. **A**. Similar BF under predrug and drug conditions. **B**. BIC shifted the BF downward in layers III and IV. **C**. BIC stabilized the BF at values below the predrug condition for all layers.

± 3.9 ms, $n = 49$) and was not significantly different across layers ($p > 0.05$, Kruskal–Wallis test).

Change of tuning caused by $GABA_A$ blockade. A possible layer specificity of Q_{10dB} and Q_{40dB} values during control conditions was tested for single units, multiple units, and all units grouped together (Table 1). However, no layer specificity ($p > 0.05$, Kruskal–Wallis test) could be detected. To investigate a possible layer-specific strength of inhibition, the changes of the Q_{10dB} and Q_{40dB} values caused by $GABA_A$ blockade were plotted as a function of the cortical depth for single and multiple units (Fig. 6A). The criterion that was used to define an increase or a decrease of tuning sharpness was a change of the Q_{10dB} value of at least ±0.5 or at least ±0.125 for the Q_{40dB} value. Abolishing $GABA_A$-receptor-mediated inhibition resulted in a decrease of tuning sharpness measured as Q_{10dB} values in 45% ($n = 127$) of the units and an increase in 22% of the units. There was no evident layer specificity. A more uniform effect of blocking $GABA_A$ receptors was observed for the Q_{40dB} values: They decreased in 63% of the 110 units for which a Q_{40dB} was definable before and during BIC application and increased in only 10%. The decrease of the Q_{40dB}, and, hence, the decrease of tuning sharpness, was largest for one unit at the border of layers III and IV and for units in layer VI. However, over the whole population, there was no significant layer-specificity ($p > 0.05$, Kruskal–Wallis test).

To investigate a possible frequency asymmetry of inhibitory effects, the shifts of the high- and low-frequency slopes of the tuning curves 40 dB above the threshold were measured (Fig. 6B). The shifts were not dependent on the BF of the unit (data not shown). To take into account slight irregularities of the edges of the tuning curves, a criterion of 0.25 octave was used to define a significant shift of the slope. In the pooled data, BIC shifted the low-frequency slope in the majority of units (56%, $n = 110$) to lower frequencies (range = −3.63 to −0.25 octave) and the high-frequency slope to higher frequencies (43%, range = 0.26 to 1.68 octaves). A broadening of the tuning curve on both the high-frequency side and the low-frequency side of more than 0.25 octave was observed in 29% of the units. In 26% of the units, a pronounced broadening was observed only on the low-frequency side. Seventy-two percent of these units shifted their high-frequency slope to higher frequencies, 28% to lower frequencies. In 15% there was a pronounced broadening at only the high-frequency flank; 56% of these units shifted their low-frequency side to lower frequencies and 44% to higher frequencies. In general, the broadening toward lower frequencies was seen in a higher percentage of the neuronal sample and it was more pronounced, indicating a more widespread inhibition at the low-frequency side of the tuning curves. There was no significant layer difference in the effect of BIC on the change of the low-frequency slope ($p > 0.05$,

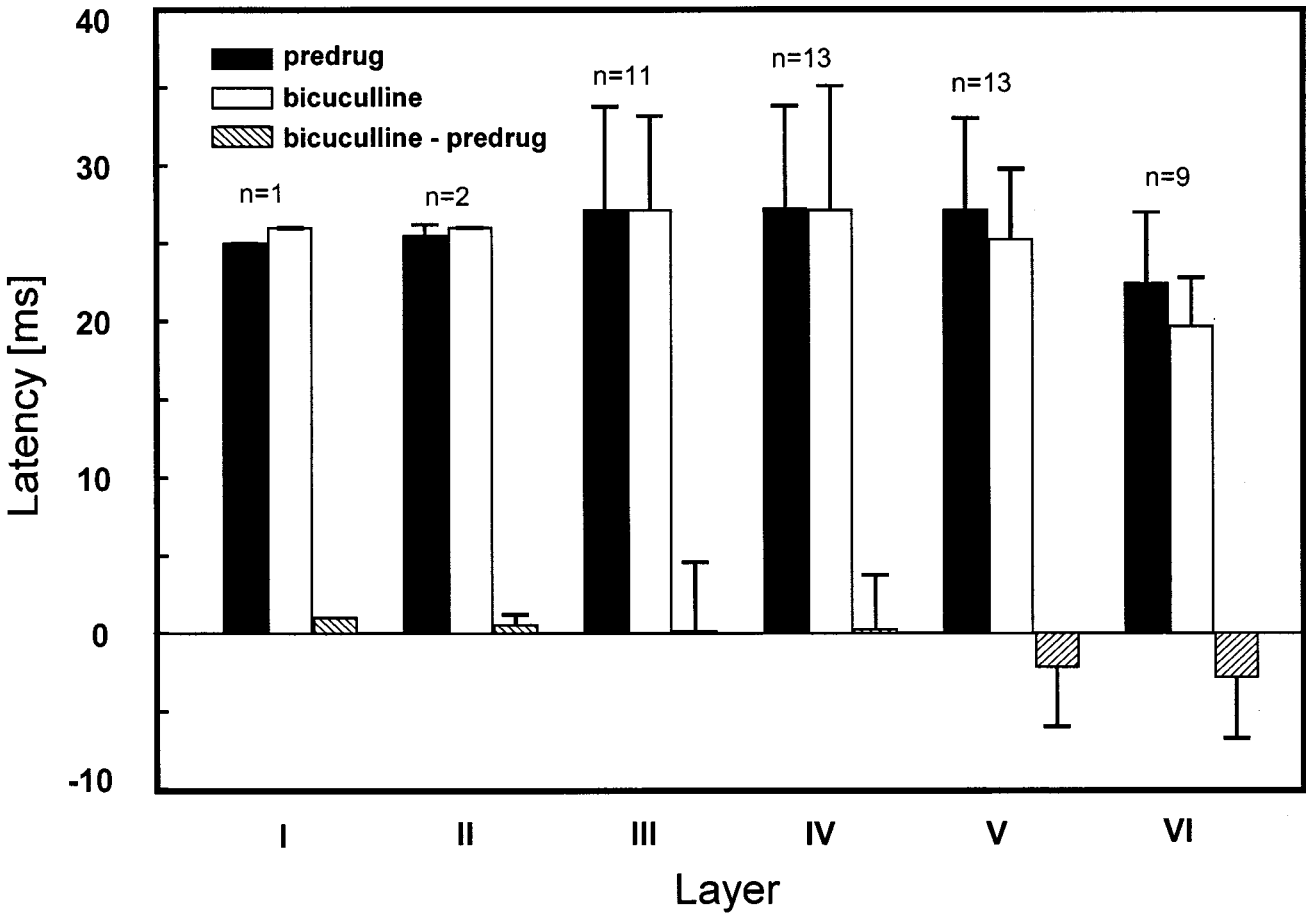

FIG. 5. Average response latencies of single units for all layers before (filled boxes) and during (open boxes) the application of BIC. Stippled boxes represent the average difference between drug and predrug latencies. Error bars represent standard deviations.

TABLE 1

Q_{10dB} and Q_{40dB} of single and multiple units per layer

	Q_{10dB}			Q_{40dB}		
Layer	*Median*	*1st quartile*	*3rd quartile*	*Median*	*1st quartile*	*3rd quartile*
I	1.12	0.87	2.02	0.89	0.64	1.30
II	1.80	1.47	4.15	0.45	0.40	0.88
III	2.28	1.60	3.91	0.65	0.52	1.19
IV	2.23	1.47	3.09	1.03	0.65	1.34
V	2.28	1.31	2.92	0.90	0.51	1.33
VI	2.31	1.53	3.01	0.88	0.49	1.54

Kruskal–Wallis test) and high-frequency slope (one-way ANOVA with Bonferroni correction).

Paradoxical effects of bicuculline and silent neurons. We recorded two single units and eight multiple units in layer I at a depth of 10–100 μm. Interestingly, for four of ten units in layer I, the application of BIC resulted in an inhibitory effect on both the stimulus-evoked discharge rate and the spontaneous rate and/or a decrease of receptive field size (Fig. 7). A small network consisting of two inhibitory neurons connected in series and projecting to the recorded unit could be responsible for this effect if BIC preferentially affects the synapses between the two inhibitory neurons. Since neuronal cell bodies are spaced far apart from each other in layer I, it is surprising that multiple-unit recordings are possible in this layer. However, spike amplitudes generally were quite small in layer I. Consequently, fluctuations of spike amplitude which led to a classification of the unit as a multiple-unit recording could have been due to the low signal-to-noise ratio. To maintain a similar classification scheme over all recordings, we still defined these units as multiple units. Of course, from the anatomical data, it can be suspected that the spike amplitude fluctuations were probably a consequence of the low signal-to-noise ratio and were not due to the presence of neighboring neurons.

Eight of 33 units recorded in layer VI and one unit at the border of layers II and III could not be driven by stimulation with pure tones under predrug conditions

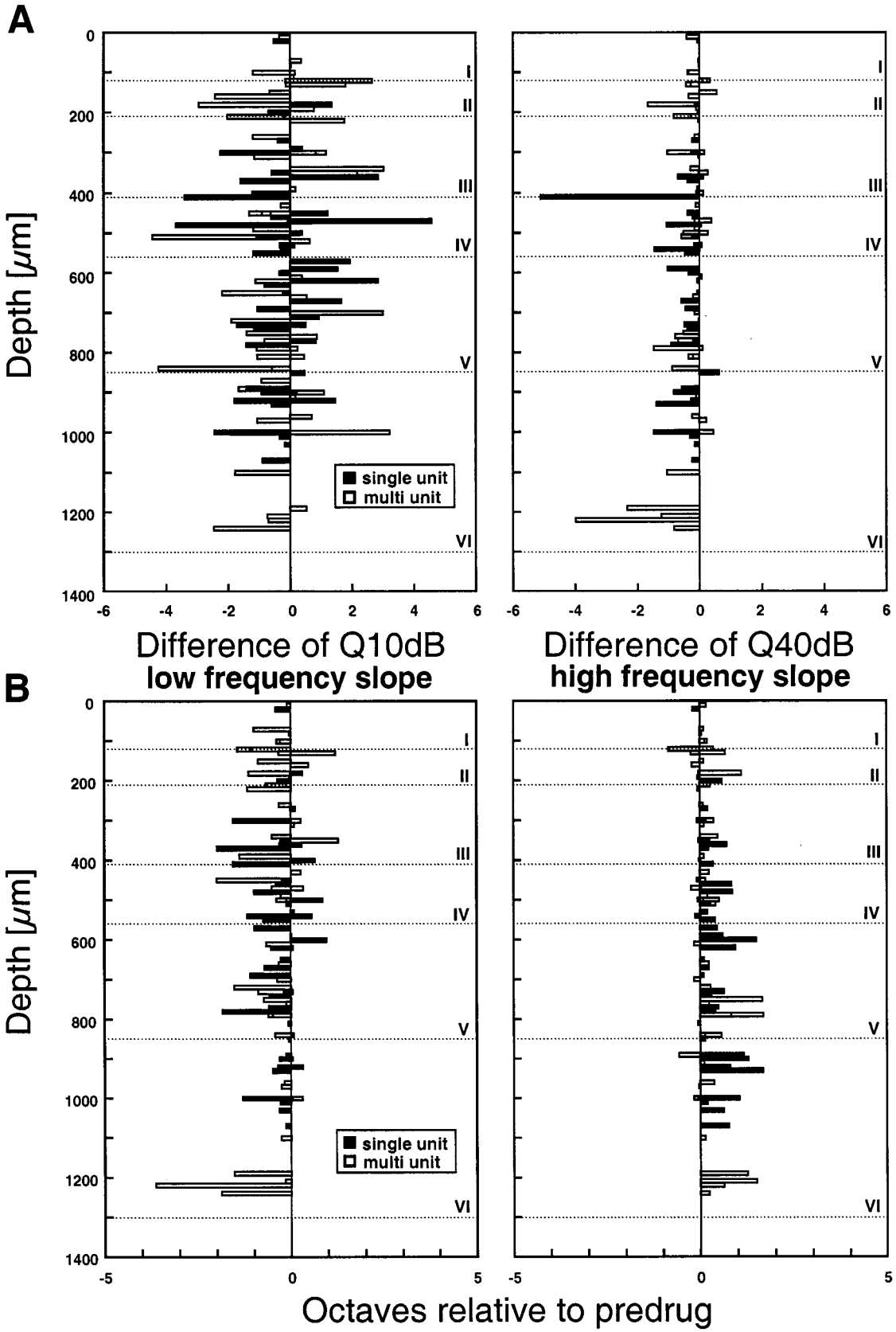

FIG. 6. **A**. Difference of Q values between predrug condition and BIC application as a function of cortical depth. BIC reduced the Q_{40dB}. **B**. Frequency shift of the low- and the high-frequency slope of the tuning curves during the application of BIC relative to the corresponding frequency of the tuning curve before drug application. Measurements were taken 40 dB above threshold.

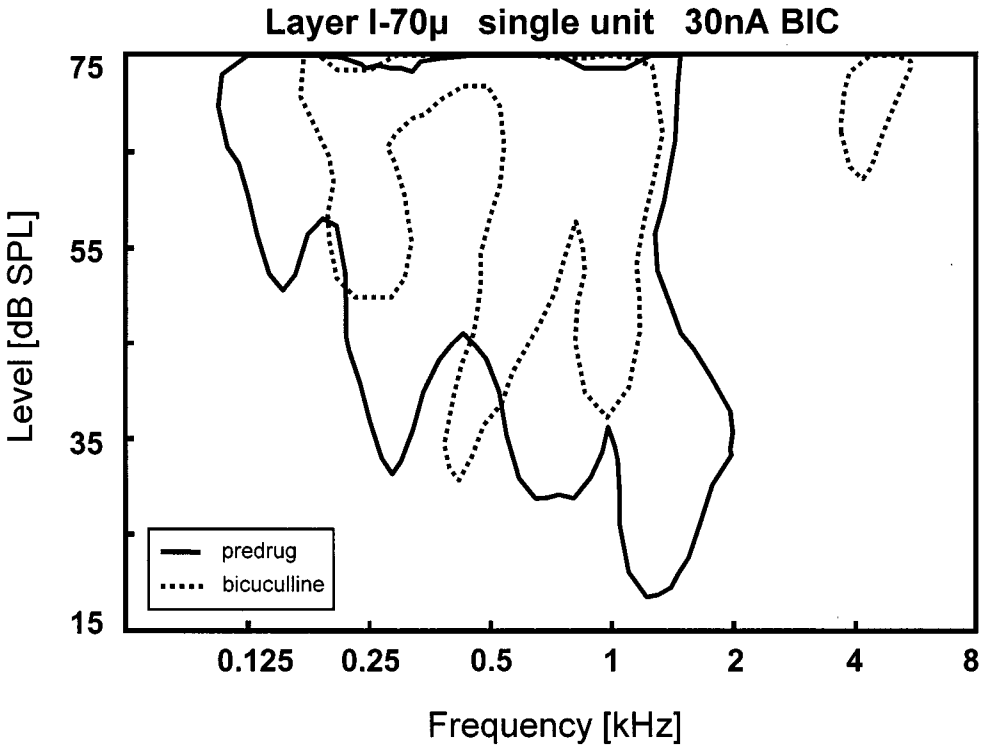

FIG. 7. Example for a sharpening of the receptive field during the application of BIC (30 nA; dashed line) for a single unit in layer I.

but showed acoustic responses within defined receptive fields during BIC application (Fig. 8). Analogous to recordings from the somatosensory cortex (Dykes et al. 1984), we defined these cells as silent neurons.

Immunocytochemistry

Figures 9A and B show the laminar distribution of GABA-immunoreactive neuronal elements. The same section was plotted twice with different contrasts to illustrate either unstained cell bodies (Fig. 9A) or GABA-immunopositive puncta (axon terminals, Fig. 9B). GABA-labeled neurons were easily distinguished from background. GABA-labeled cells and puncta (Figs. 9B and 10) were present in all cortical layers. A variety of somatic shapes and sizes (area between 39 and 205 μm^2) was observed for GABA-labeled neurons. A classification of cells was not possible because only the most proximal dendritic pattern was visible. GABAergic neurons constituted 14.8% of the neurons located in the auditory cortex. The proportion of GABA-labeled neurons was similar across layers II, III, IV, and VI and was largest in layers I (36.1%) and V (15.3%, Fig. 9C *top*). The density of GABA-labeled axon terminals seemed to be highest in layer V (see Fig. 9B). To examine the laminar distribution of GABA-immunoreactive axosomatic endings, the number of puncta on somata of 8–22 cells per layer was counted. Immunonegative nonpyramidal cells in layers I and IV and immunonegative pyramidal cells in the remaining layers were investigated. Pyramidal cells in layer V received the highest number of axosomatic endings (average = 12.1 ± 3.7, Fig. 9C *middle*) which often extended along the proximal dendrites (see Fig. 10). There were no layer-specific differences in the number of puncta per cell perimeter (Fig. 9C *bottom*).

DISCUSSION

Methodological consideration

The diffusion range of BIC can extend up to 400 μm. This implies that in those parts of our experiments where larger injection currents were used, BIC could have exceeded laminar boundaries, especially in the upper layers. The resulting effect of BIC application, therefore, can reflect the sum of activity caused by blockade of $GABA_A$ receptors located on neuronal elements near the recording site as well as on neurons in layers adjacent to the recording site. Additionally, it has to be kept in mind that neurons in different layers differ in their somatic shape and dendritic tree geometry. Typical pyramidal neurons integrate inhibition from several spatially separated input regions, e.g., they send the apical dendrite to layer I where its terminal tuft receives inhibitory input which can not be

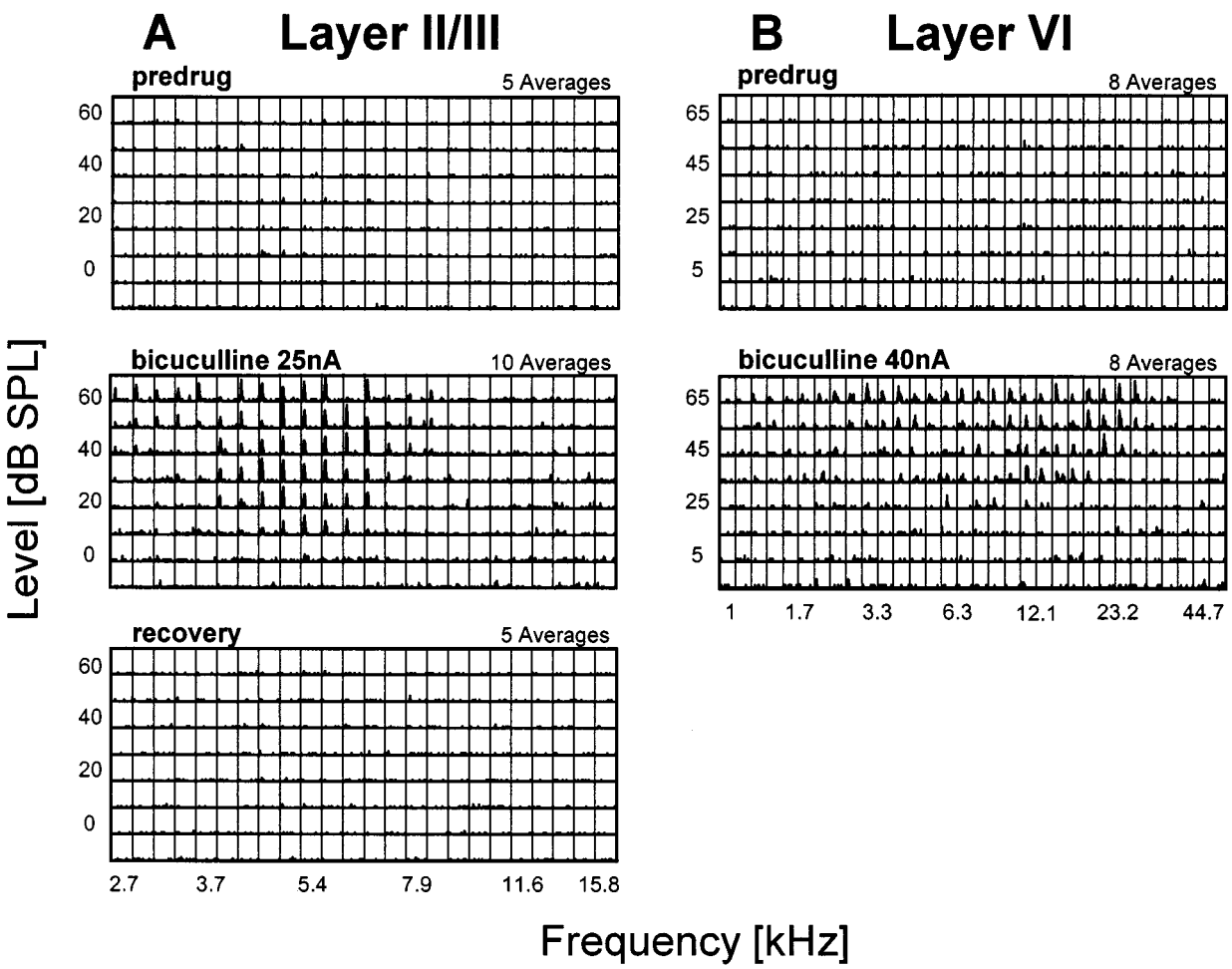

FIG. 8. Receptive fields of a single unit in layer II/III (**A**) and a multiple unit in layer VI (**B**) composed of single PSTHs. Prior to BIC application, there was no obvious response to pure tone stimuli and a receptive field could not be defined. PSTH bin width is 4 ms. PSTH *y* axis is 15 spikes (**A**) and 10 spikes (**B**).

assessed by local pharmacological application close to the cell body. Therefore, inhibition might be even more complex than demonstrated in this study. Pharmacological manipulation of inhibition in the different cortical layers while recording from one neuron in a specific layer might reveal the whole extent of inhibitory interactions in a cortical column.

Comparison of pharmacological blocking of GABA with other studies

The observation that the blockade of $GABA_A$ receptors led to a pronounced increase of neuronal firing, even in the absence of sound, shows that $GABA_A$ receptors were tonically activated by the release of GABA and that these receptors were involved in the regulation of neuronal activity. The change of receptive field size was analyzed for units in which an increase of discharge and/or spontaneous activity was observed. The pharmacologically induced loss of inhibition allowed expression of excitatory inputs from frequencies which were originally not apparent as part of the excitatory field of a given unit because they were masked by the inhibition.

Sharpening of frequency tuning curves by GABAergic inhibition takes place at different levels in the auditory system as demonstrated in pharmacological studies (e.g., dorsal cochlear nucleus of the rat: Yajima and Hayashi 1990; inferior colliculus of bats: Vater et al. 1992; Yang et al. 1992; Klug and Pollak 2000; medial geniculate body of the mustached bat: Suga et al. 1997; auditory cortex analogue in the bird: Müller and Scheich 1988). Comparable to data of Wang et al. (2000) in A1 of the chinchilla, we could show that intracortical GABAergic inhibition was involved in sharpening the receptive field in the majority of the A1 units. In our data, the effects of BIC on the receptive fields were most obvious in a lowering of the Q_{40dB} values. This indicates that inhibitory mechanisms are mainly effective at moderate or higher stimulus levels. GABA-mediated inhibitory sidebands were present at both the high- and the low-frequency flanks of the

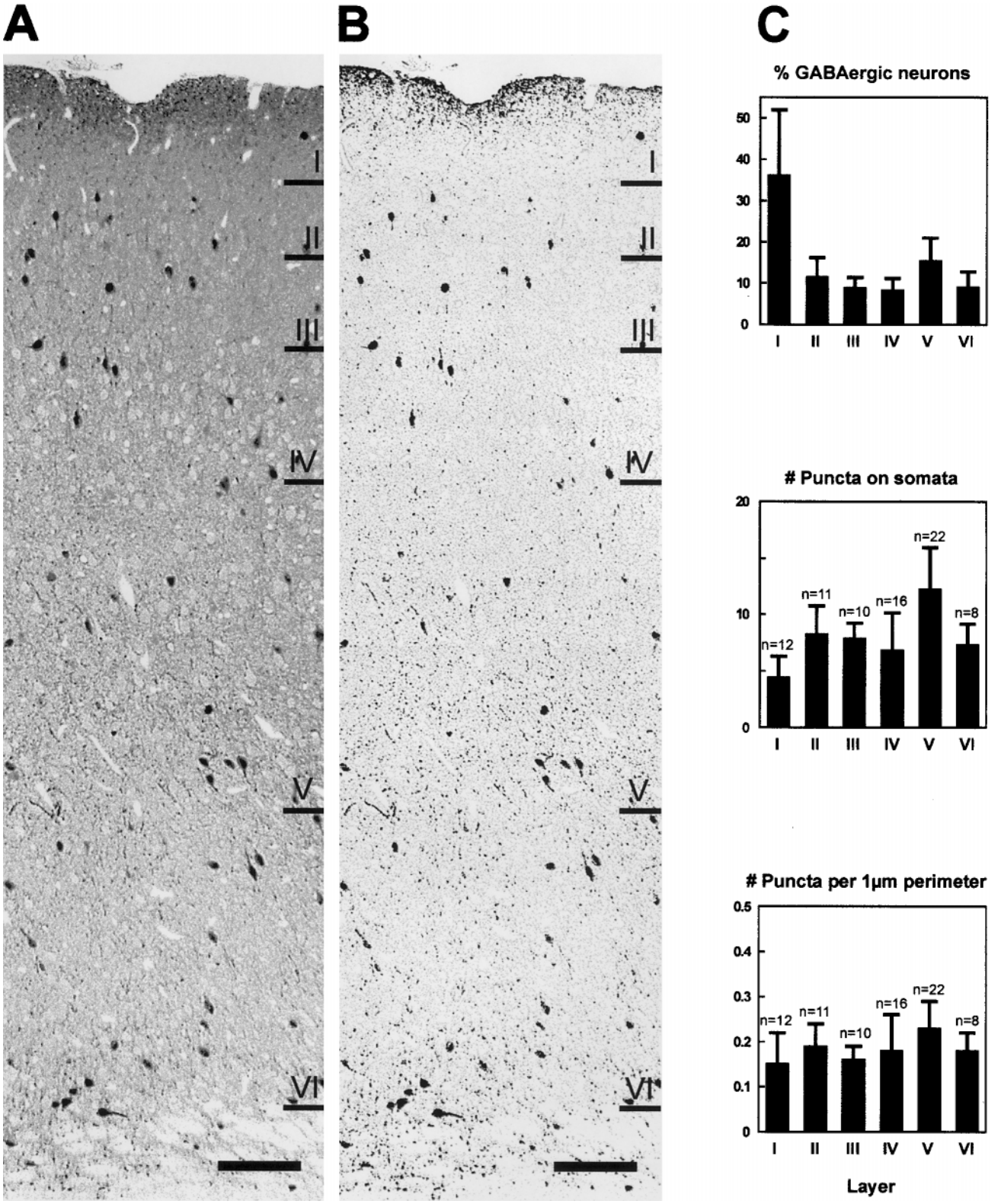

FIG. 9. **A**, **B**. GABA-immunostained 1-μm-thick section of the auditory cortex, plotted twice with different contrast enhancement (Adobe Photoshop), to show the profiles of immunopositive and immunonegative neurons (**A**) or immunopositive neurons and axon terminals (puncta, **B**). The immunonegative cells were often ringed by immunopositive endings. The density of puncta seemed to be highest in layer V. N.A. 0.7, $\times$40. Scale bar = 100 μm. **C**. Numerical analysis of GABAergic neurons and axon terminals. *Top:* Histogram showing the laminar distribution of GABAergic neurons. Error bars represent standard errors of the average of 12 samples from one animal. *Middle:* Histogram showing the numbers of puncta on somata of immunonegative neurons. Error bars represent standard errors. For further explanation see text. *Bottom:* Histogram showing the density of puncta on cell perimeter. Error bars represent standard errors.

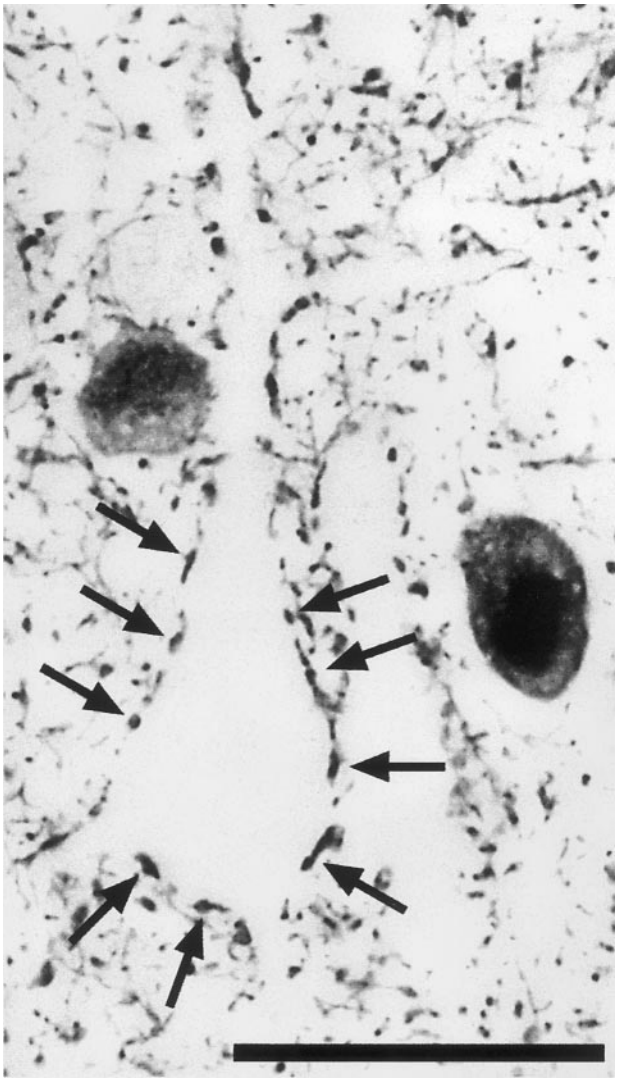

FIG. 10. An immunonegative pyramidal cell in layer V whose soma and dendritic trunk received many GABAergic puncta (arrows). N.A. 1.25, ×100, oil immersion. Scale bar = 25 μm.

excitatory tuning curve in 29% of the units. The higher percentage of neurons in the chinchilla A1 (61% out of 36 neurons) that showed an expansion along both sides of the tuning curves could be related to a generally more narrow tuning in the chinchilla A1. However, direct comparison with our data is difficult since Wang et al. (2000) did not provide sufficiently detailed information about their threshold criterion. In contrast to our findings, a study by Schulze and Langner (1999), which investigated the processing of amplitude modulation, did not show a significant expansion of the frequency response range measured 30 dB above threshold during the application of BIC in the gerbil A1. Our data would suggest that, at this stimulus level, inhibitory influence is prominent in many units. The discrepancy between our data and the results of Schulze and Langner (1999) could result from differences in the methodological procedures concerning iontophoresis or reflect a sampling bias since they tested the effect of BIC on receptive fields in only 23 units that were taken exclusively from the low-frequency region of A1.

Effect of pharmacological blocking of GABA compared with two-tone masking in the auditory cortex

An enlargement of receptive fields of auditory cortex neurons has also been shown in two-tone masking studies (e.g., Shamma and Symmes 1985; Sutter and Schreiner 1991; Shamma et al. 1993; Calford and Semple 1995; Brosch and Schreiner 1997; Sutter et al. 1999). In our study, the percentage of tuning curves with symmetric inhibitory sidebands is in the range of data from two-tone masking studies where 30% (ferret: Shamma et al. 1993) and 38% (cat: Sutter et al. 1999) of the neurons showed an inhibitory sideband on both the high- and the low-frequency flanks of the tuning curve. In the latter study, the inhibitory areas ranged from a single inhibitory band to more than four inhibitory regions. Cells with the simple two-band inhibitory structure were more common in the ventral part of the cat A1, corresponding to an increased tuning sharpness, the high degree of nonmonotonicity, and a high percentage of GABAergic neurons found in this cortical area (Schreiner and Mendelson 1990; Schreiner et al. 1992; Prieto et al. 1994a; for review: Ehret 1997). Tuning curves with complex structure were more common in the dorsal A1 and related to the higher percentage of multipeaked and broadly tuned neurons in this cortex region. Information about a similar functional organization in the gerbil is not yet available. From two-tone masking studies, there is evidence that the bands between the excitatory areas are caused by inhibition. Since in our study multipeaked tuning curves could be converted to single-peaked tuning curves by the local application of BIC, we suggest that intracortical $GABA_A$-mediated inhibition plays an important role in producing these inhibitory bands and, hence, multipeaked tuning curves.

In the present study, the extent of the expansion of up to 3.6/1.68 octaves at the low-/high-frequency side is basically similar to that reported by Shamma and Symmes (1985) for the squirrel monkey. However, it needs to be kept in mind that two-tone masking measures a net suppressive effect which includes mechanical suppression in the cochlea and inhibitory actions at all levels of the auditory system. Furthermore, the degree of two-tone inhibition strongly depends on several stimulation parameters, e.g., the timing between the stimuli and the position of the

fixed stimulus in respect to the excitatory response area (Calford and Semple 1995; Brosch and Schreiner 1997; Brosch et al. 1999). A direct comparison of the effect of pharmacological compounds that modify intracortical inhibition with the influence of two-tone masking in individual neurons could elucidate the relative contribution of intracortical and subcortical inhibitory mechanisms in shaping auditory tuning curves.

Is there a layer-specific strength of inhibition?

In the auditory cortex of the gerbil, an increased tuning sharpness in layers III and IV has been reported (Sugimoto et al. 1997). This could have been caused by the specific input from neurons of the ventral division of the medial geniculate body which are known to be sharply tuned, e.g., in the cat (for review: Clarey et al. 1992). The broad tuning in layers I and VI could be caused by diffuse inputs from the medial division of the medial geniculate body (Sugimoto et al. 1997). In the present study, we could not observe a layer-dependent change of tuning sharpness as quantified by Q_{10dB} and Q_{40dB} values. The most likely reason for the discrepancy of our data with that of Sugimoto et al. (1997) could be the methodological difference in defining tuning curves. In contrast to Sugimoto et al. (1997), who defined tuning curves using an audio–visual method, we used random stimulus presentations to measure a detailed response area. From the corresponding response area, the tuning curves were then calculated by a software program which took into account a standardized threshold criterion. The whole procedure yielded tuning curves which, in comparison to those of Sugimoto et al. (1997), were more complex and also slightly broader. Indications that the tuning characteristics are independent of cortical depth have also been found for the bat (Chen and Jen 2000), mouse (Shen et al. 1999), and cat auditory cortex (Abeles and Goldstein 1970).

Our neurophysiological data showed that the strength of inhibition, as quantified in comparison of several response parameters in predrug conditions and GABA blockade, was not significantly layer-dependent. This is consistent with data of a recent study (Chen and Jen 2000) that showed a similarity of the expanded tuning curves measured during BIC application within an orthogonal penetration in the auditory cortex of a bat species. The high percentage of silent neurons that we found in layer VI suggests that inhibition is strong in the deep layers of A1, which is similar to data from the somatosensory cortex (Dykes et al. 1984).

The percentage of GABAergic neurons found in the gerbil (15%) is between that reported for the cat (24.6%; Prieto et al. 1994a) and the ferret auditory cortex (10.4%; Gao et al. 1999). The proportion of GABAergic neurons appears to be species-specific, since values for sensory cortical areas of the ferret are generally lower than reported for cat neocortex. In cat A1, the percentage of GABAergic neurons peaks in layers I and V, which is comparable to our data. However, the respective percentages are higher in the cat, especially in layer I. Since most neurophysiological data are from pyramidal cells in layers II, III, V, and VI, we counted puncta on pyramidal cells in these layers. The number of puncta was highest for layer V pyramidal cells. However, one has to take into account the larger somatic size of these cells. Indeed, when the number of puncta was related to the cell perimeter, no significant difference was found across layers.

In the neurophysiological data, we found no layer-specific effects of inhibition, except for a high percentage of silent neurons in layer VI. With our method we mainly measured inhibition mediated by GABAergic synapses on the cell soma and, therefore, could not assess a possible layer-specificity of more distant dendritic inhibitory synapses.

Potential functional role of silent neurons in the auditory cortex

In some units that did not respond to pure tones under control conditions, we observed that BIC elicited auditory responses that were frequency-tuned. These neurons were silent, not because of a lack of excitatory input, but because a tonic $GABA_A$-receptor-mediated inhibition completely suppressed their ability to respond to pure tone stimuli. Silent neurons were also reported in the inferior colliculus of horseshoe bats (Vater et al. 1992), in the bird auditory cortex analogue (Müller and Scheich 1987), and in cat somatosensory cortex (Dykes et al. 1984). One could argue that anesthesia could lead to a change of response pattern and possibly to a complete suppression of neuronal activity of neurons. However, in the case of our anesthetic (ketamine/xylazine), a possible change of the response pattern would most probably not be caused by an influence on GABAergic receptors but, if at all, by a blockade of glutaminergic receptors (NMDA receptors). The strongest argument against the possibility that silent neurons are due to a general effect of anesthesia is the fact that such neurons were almost exclusively found in the deep layers. This property implies a more specific physiological response characteristic inherent to the neurons. Similar to our data, Dykes et al. (1984) found silent neurons mainly in superficial and deeper layers. Dykes et al. (1984) routinely applied glutamate to isolate neurons in all layers and to detect silent neurons in the somatosensory cortex of the cat. We usually did not apply glutamate to search for neurons and, consequently, in the present

study silent neurons might be underrepresented. Therefore, the percentage of silent neurons in layer VI might be even higher suggesting that tonic inhibition is remarkably pronounced in this layer. In our study, most of these neurons were found in layer VI. Neurons in layers VI project to the thalamus, to secondary auditory areas, or to the contralateral cortex. They represent major output neurons of the cortex, and it may be of functional significance that their activity can be completely switched off by appropriate GABAergic inhibition.

ACKNOWLEDGMENTS

We thank G. Neuweiler and two anonymous reviewers for their critical comments on the manuscript and C. Kapfer for helpful discussion. This study was supported by the DFG, Forschergruppe Hoerobjekte. The experiments reported here are in accordance with the declaration of Helsinki and with the animal experimental approval (Regierung von Oberbayern: AZ 211-2531-37/98).

REFERENCES

ABELES M, GOLDSTEIN MH. Functional architecture in cat primary auditory cortex: Columnar organization and organization according to depth. J. Neurophysiol. 33:172–187, 1970.

AVOLI M, MATTIA D, SINISCALCHI A, PERREAULT P, TOMAIUOLO F. Pharmacology and electrophysiology of a synchronous GABA-mediated potential in the human neocortex. Neuroscience 62:655–666, 1994.

BARTH DS, DI S. Three-dimensional analysis of auditory-evoked potentials in rat neocortex. J. Neurophysiol. 64:1527–1536, 1990.

BROSCH M, SCHREINER CE. Time course of forward masking tuning curves in cat primary auditory cortex. J. Neurophysiol. 77:923–943, 1997.

BROSCH M, SCHULZ A, SCHEICH H. Processing of sound sequences in macaque auditory cortex: response enhancement. J. Neurophysiol. 82:1542–1559, 1999.

CALFORD MB, SEMPLE MN. Monaural inhibition in cat auditory cortex. J. Neurophysiol. 73:1876–1891, 1995.

CHEN QC, JEN PH-S. Bicuculline application affects discharge patterns, rate-intensity functions, and frequency tuning characteristics of bat auditory cortical neurons. Hear. Res. 150:161–174, 2000.

CLAREY JC, BARONE P, IMIG TJ. Physiology of thalamus and cortex. In: Popper AN, Fay RR, (eds) The mammalian auditory pathway: Neurophysiology. Springer-Verlag, New York, 1992, 232–334.

CROOK JM, KISVARDAY ZF, EYSEL UT. Evidence for a contribution of lateral inhibition to orientation tuning and direction selectivity in cat visual cortex: reversible inactivation of functionally characterized sites combined with neuroanatomical tracing techniques. Eur. J. Neurosci. 10:2056–2075, 1998.

DYKES RW, LANDRY P, METHERATE R, HICKS TP. Functional role of GABA in cat primary somatosensory cortex: Shaping receptive fields of cortical neurons. J. Neurophysiol. 52:1066–1093, 1984.

EHRET G. The auditory cortex. J. Comp. Physiol. 181:547–557, 1997.

GAO WJ, NEWMAN DE, WORMINGTON AB, PALLAS SL. Development of inhibitory circuitry in visual and auditory cortex of postnatal ferrets: immunocytochemical localization of GABAergic neurons. J. Comp. Neurol. 409:261–273, 1999.

HAVEY DC, CASPARY DM. A simple technique for constructing piggy back multibarrel electrodes. Electroencephalogr. Clin. Neurophysiol. 48:249–251, 1980.

HICKS TP. Antagonism of synaptic transmission *in vivo:* contributions of microiontophoresis. Brain Behav. Evol. 22:1–12, 1983.

HORIKAWA J, HOSOKAWA Y, KUBOTA M, NASU M, TANIGUCHI I. Optical imaging of spatiotemporal patterns of glutamatergic excitation and GABAergic inhibition in the guinea-pig auditory cortex *in vivo*. J. Physiol. 497:629–638, 1996.

IMIG TJ, ADRIAN HO. Binaural columns in the primary field (A1) of cat auditory cortex. Brain Res. 138:241–257, 1977.

IMIG TJ, RUGGERO MA, KITZES LM, JAVEL E, BRUGGE JF. Organization of auditory cortex in the owl monkey (*Aotus trivirgatus*). J. Comp. Neurol. 171:111–128, 1977.

KEMMER M, VATER M. The distribution of GABA and glycine immunostaining in the cochlear nucleus of the mustached bat (*Pteronotus pamellii*). Cell Tissue Res. 287:487–506, 1997.

KLUG A, POLLAK G. Responses of many IC neurons to complex stimuli can be predicted based on their excitatory and inhibitory tuning. Assoc. Res. Otolaryngol. Abstr. 883, 2000.

KOLSTON J, OSEN KK, HACKNEY CM, OTTERSEN OP, STORM–MATHISEN J. An atlas of glycine- and GABA-like immunoreactivity and colocalization in the cochlear nuclear complex of the guinea pig. Anat. Embryol. 186:443–465, 1992.

KYRIAZI HT, CARVELL GE, BRUMBERG JC, SIMONS DJ. Quantitative effects of GABA and bicuculline methiodide on receptive field properties of neurons in real and simulated whisker barrels. J. Neurophysiol. 75:547–560, 1996.

LIU CJ, GRANDES P, MATUTE C, CUENOD M, STREIT P. Glutamate-like immunoreactivity revealed in rat olfactory bulb, hippocampus and cerebellum by monoclonal antibody and sensitive staining method. Histochemistry 90:427–445, 1989.

MERZENICH MM, KNIGHT PL, ROTH GL. Representation of cochlea within primary auditory cortex in the cat. J. Neurophysiol. 38:231–249, 1975.

MITANI A, SHIMOKOUCHI M, ITOH K, NOMURA S, KUDO M, MIZUNO N. Morphology and laminar organization of electrophysiologically identified neurons in the primary auditory cortex in the cat. J. Comp. Neurol. 235:430–447, 1985.

MOUNTCASTLE VB. The columnar organization of the neocortex. Brain 120:701–722, 1997.

MÜLLER CM, SCHEICH H. GABAergic inhibition increases the neuronal selectivity to natural sounds in the avian auditory forebrain. Brain Res. 414:376–380, 1987.

MÜLLER CM, SCHEICH H. Contribution of GABAergic inhibition to the response characteristics of auditory units in the avian forebrain. J. Neurophysiol. 59:1673–1689, 1988.

OONISHI S, KATSUKI Y. Functional organization and integrative mechanism on the auditory cortex of the cat. Jpn. J. Physiol. 15:342–365, 1965.

PELLEG–TOIBA R, WOLLBERG Z. Tuning properties of auditory cortex cells in the awake squirrel monkey. Exp. Brain Res. 74:353–364, 1989.

PHILLIPS DP, IRVINE DR. Some features of binaural input to single neurons in physiologically defined area A1 of cat cerebral cortex. J. Neurophysiol. 49:383–395, 1983.

PRIETO JJ, PETERSON BA, WINER JA. Morphology and spatial distribution of GABAergic neurons in cat primary auditory cortex (A1). J. Comp. Neurol. 344:349–382, 1994a.

PRIETO JJ, PETERSON BA, WINER JA. Laminar distribution and neuronal targets of GABAergic axon terminals in cat primary auditory cortex (A1). J. Comp. Neurol. 344:383–402, 1994b.

RICHTER K, HESS A, SCHEICH H. Functional mapping of transsynaptic effects of local manipulations of inhibition in gerbil auditory cortex. Brain Res. 831:184–199, 1999.

SALLY SL, KELLY JB. Organization of auditory cortex in the albino rat: Sound frequency. J. Neurophysiol. 59:1627–1638, 1988.

SCHREINER CE, MENDELSON JR. Functional topography of cat primary auditory cortex: distribution of integrated excitation. J. Neurophysiol. 64:1442–1459, 1990.

SCHREINER CE, MENDELSON JR, SUTTER ML. Functional topography of cat primary auditory cortex: representation of tone intensity. Exp. Brain Res. 92:105–122, 1992.

SCHULZE H, LANGNER G. Auditory cortical responses to amplitude modulations with spectra above frequency receptive fields: evidence for wide spectral integration. J. Comp. Physiol. 185:493–508, 1999.

SHAMMA SA, SYMMES D. Patterns of inhibition in auditory cortical cells in awake squirrel monkeys. Hear. Res. 19:1–13, 1985.

SHAMMA SA, FLESHMAN JW, WISER PR, VERSNEL H. Organization of response areas in ferret primary auditory cortex. J. Neurophysiol. 69:367–383, 1993.

SHEN JX, XU ZM, YAO YD. Evidence for columnar organization in the auditory cortex of the mouse. Hear. Res. 137:174–177, 1999.

SILLITO AM. Functional considerations of the operation of GABAergic inhibitory processes in the visual cortex. In: Jones EG, Peters A, (eds) Cerebral Cortex, Vol. 2, Plenum, New York, 1984, 91–114.

SUGA N, JEN PHS. Disproportionate tonotopic representation for processing CF-FM sonar signals in the mustache bat auditory cortex. Science 194:542–544, 1976.

SUGA N, ZHANG Y, YAN J. Sharpening of frequency tuning by inhibition in the thalamic auditory nucleus of the mustached bat. J. Neurophysiol. 77:2098–2114, 1997.

SUGIMOTO S, SAKURADA M, HORIKAWA J, TANIGUCHI I. The columnar and layer-specific response properties of neurons in the primary auditory cortex of Mongolian gerbils. Hear. Res. 112:175–185, 1997.

SUTTER ML, SCHREINER CE. Physiology and topography of neurons with multipeaked tuning curves in cat primary auditory cortex. J. Neurophysiol. 65:1207–1226, 1991.

SUTTER ML, SCHREINER CE, MCLEAN M, O'CONNER KN, LOFTUS WC. Organization of inhibitory frequency receptive fields in cat primary auditory cortex. J. Neurophysiol. 82:2358–2371, 1999.

TAMÁS G, BUHL EH, LÖRINCZ A, SOMOGYI P. Proximally targeted GABAergic synapses and gap junctions synchronize cortical interneurons. Natl. Neurosci. 3:366–371, 2000.

THOMAS H, TILLEIN J, HEIL P, SCHEICH H. Functional organization of auditory cortex in the mongolian gerbil (*Meriones unguiculatus*). I. Electrophysiological mapping of frequency representation and distinction of fields. Eur. J. Neurosci. 5:882–897, 1993.

VATER M. Ultrastructural and immunocytochemical observations on the superior olivary complex of the mustached bat. J. Comp. Neurol. 358:155–180, 1995.

VATER M, HARTMANN H, KÖSSL M, GROTHE B. The functional role of GABA and glycine in monaural and binaural processing in the inferior colliculus of horseshoe bats. J. Comp. Physiol. 171:541–553, 1992.

VOLKOV IO, GALAZJUK AV. Formation of spike response to sound tones in cat auditory cortex neurons: interaction of excitatory and inhibitory effects. Neuroscience 43:307–321, 1991.

WANG J, CASPARY DM, SALVI RJ. GABA-A antagonist causes dramatic expansion of tuning in primary auditory cortex. Neuroreport 11:1137–1140, 2000.

WINER JA. The functional architecture of the medial geniculate body and the primary auditory cortex. In: Popper AN, Fay RR, (eds) The mammalian auditory pathway: Neuroanatomy. Springer-Verlag, New York, 1992, 222–409.

YAJIMA Y, HAYASHI Y. GABAergic inhibition upon auditory response properties of neurons in the dorsal cochlear nucleus of the rat. Exp. Brain Res. 81:581–588, 1990.

YANG L, POLLAK GD, RESLER C. GABAergic circuits sharpen tuning curves and modify response properties in the mustache bat inferior colliculus. J. Neurophysiol. 68:1760–1774, 1992.